Developmental Biology 450 (2019) 34–46

Contents lists available at ScienceDirect

Developmental Biology

journal homepage: www.elsevier.com/locate/developmentalbiology

Roles of Polycomb group proteins Enhancer of zeste (E(z)) and Polycomb (Pc) during metamorphosis and larval leg regeneration in the flour beetle *Tribolium castaneum*

Jacquelyn Chou [1], Alex C. Ferris [1,2], Teresa Chen, Ruth Seok, Denise Yoon, Yuichiro Suzuki [*]

Department of Biological Sciences, Wellesley College, 106 Central St., Wellesley, MA 02481, USA

ARTICLE INFO

Keywords:
Limb regeneration
Metamorphosis
Tribolium castaneum
Polycomb group (PcG) proteins
Epigenetics
H3K27
Enhancer of zeste (E(z))
Polycomb
Homeotic transformation

ABSTRACT

Many organisms both undergo dramatic morphological changes during post-embryonic development and also regenerate lost structures, but the roles of epigenetic regulators in such processes are only beginning to be understood. In the present study, the functions of two histone modifiers were examined during metamorphosis and larval limb regeneration in the red flour beetle *Tribolium castaneum*. *Polycomb* (*Pc*), a member of Polycomb repressive complex 1 (PRC1), and *Enhancer of zeste* (*E(z)*), a member of Polycomb repressive complex 2 (PRC2), were silenced in larvae using RNA interference. In the absence of Pc, the head appendages of adults transformed into a leg-like morphology, and the legs and wings assumed a metathoracic identity, indicating that Pc acts to specify proper segmental identity. Similarly, silencing of *E(z)* led to homeotic transformation of legs and wings. Additional defects were also observed in limb patterning as well as eye morphogenesis, indicating that PcG proteins play critical roles in imaginal precursor cells. In addition, larval legs and antennae failed to re-differentiate when either *Pc* or *E(z)* was knocked down, indicating that histone modification is necessary for proper blastema growth and differentiation. These findings indicate that PcG proteins play extensive roles in postembryonic plasticity of imaginal precursor cells.

1. Introduction

Metamorphosis and regeneration are post-embryonic developmental processes that involve major tissue patterning and remodeling events. These processes require substantial changes in gene expression, which could be coordinated epigenetically through changes in chromatin structure (Katsuyama and Paro, 2011; Rouhana and Tasaki, 2016). Yet few studies have examined the roles of epigenetic regulators during metamorphosis and regeneration.

Insects can be categorized into three major groups that differ in the degree of morphological changes exhibited during post-embryonic development. Juveniles of ametabolous insects resemble the adults and undergo minimal external morphogenetic changes during post-embryonic development. Hemimetabolous insects also undergo relatively minor external morphogenetic changes during development except for the wings and the genitalia. In contrast, holometabolous insects undergo dramatic morphogenetic changes during metamorphosis. While studies on roles of epigenetic regulators have been conducted on imaginal discs of *Drosophila*, a holometabolous insect, very little is known about the function of epigenetic regulators in other insects, such as Tenebrionid beetles, whose larval cells – or imaginal precursor cells – can transform into adult cells and thus exhibit much plasticity (Huet and Lenoir-Rousseaux, 1976; Truman and Riddiford, 2002; Tanaka and Truman, 2005; Villarreal et al., 2015). Importantly, the *Drosophila* mode of development, where all epidermal cells are replaced by histoblast cells or imaginal disc cells, is highly derived. Most other holometabolous insects undergo a more standard mode of development, where the larval epidermal cells are retained and contribute to the adult epidermis (Snodgrass, 1954). Little is known about the roles of epigenetic regulators during metamorphosis in such species. In addition, many members of all three groups of insects are capable of regenerating their appendages (Maruzzo and Bortolin, 2013). Whether epigenetic regulators play similar roles during limb regeneration in insects with distinct developmental modes is not known. Thus, comparing the roles of epigenetic

* Corresponding author.
E-mail address: ysuzuki@wellesley.edu (Y. Suzuki).
[1] Denotes equal contribution.
[2] Current address: Department of Bioengineering, Stanford University, Stanford, CA 94305.

https://doi.org/10.1016/j.ydbio.2019.03.002
Received 17 December 2018; Received in revised form 24 February 2019; Accepted 4 March 2019
Available online 7 March 2019

regulators between these insects with distinct modes of post-embryonic development should provide insights into the regulation of cellular plasticity.

In this study, we focused on Polycomb group (PcG) proteins, which play critical roles in maintaining cellular identity and differentiation (Aloia et al., 2013; Ringrose and Paro, 2004; Sauvageau and Sauvageau, 2010; Schuettengruber et al., 2017). PcG genes are involved in stabilizing chromatin structure through histone modification and act as transcriptional repressors (Di Croce and Helin, 2013; Schuettengruber et al., 2017). At least 16 PcG proteins have been identified in *Drosophila* that participate in three separate multiprotein complexes: Polycomb repressive complex 1 (PRC1), Polycomb repressive complex 2 (PRC2) and Pho repressive complex (PhoRC). The canonical PRC1 consists of Posterior Sex Combs (Psc), Polyhomeotic (Ph), Polycomb (Pc), and dRING1 (Francis et al., 2001; Shao et al., 1999). PRC2 (Polycomb repressive complex 2) typically comprises of Enhancer of zeste (E(z)), Extra sex combs (Esc) and Suppressor of zeste 12 (Su(z)12) (Muller et al., 2002). PhoRC was identified in *Drosophila* and contains Pleiohomeotic (Pho) and Scm-related protein containing four MBT domains (Sfmbt) (Klymenko et al., 2006). PRC1 and PRC2 are best characterized, and their members and targets are highly conserved across metazoans (Schuettengruber et al., 2017).

The canonical model for PcG-mediated gene silencing involves recruitment of H3K27 methylation by PRC2, followed by chromatin compaction and gene silencing by PRC1 (Grossniklaus and Paro, 2014; Schuettengruber et al., 2017; Shao et al., 1999; Wang et al., 2004b). Specifically, a core PRC2 protein, E(z), is a histone methyltransferase that catalyzes the trimethylation of lysine 27 of histone H3 (H3K27me3) (Cao et al., 2002; Cao and Zhang, 2004; Czermin et al., 2002). The chromodomain of Pc, a component of PRC1, then binds to H3K27me3 and recruits PRC1 (Pengelly et al., 2013). At least part of PRC1 activity arises from the monoubiquitylation at lysine 119 of H2A (H2AK119) by dRING1 although H2A ubiquitination is not necessary for some functions of PRC1 (Endoh et al., 2012; Gutierrez et al., 2012; Wang et al., 2004a).

PcG proteins were first identified by Ed Lewis as critical regulators of Hox gene expression in *Drosophila* (Lewis, 1978). In vertebrates, mutations in PcG proteins have been associated with a shift in the anterior limit of Hox genes, leading to posterior transformation of the axial skeleton (Akasaka et al., 1996; Bel et al., 1998; Takihara et al., 1997; van der Lugt et al., 1994). In *Drosophila*, Hox genes are initially activated by gap genes and other segmentation genes, but maintenance of proper Hox gene expression patterns is conferred by PcG proteins. Mutations in PcG proteins lead to misexpression of Hox genes (Jurgens, 1985; McKeon and Brock, 1991; Muller and Bienz, 1991; Simon et al., 1992) and corresponding homeotic transformations (Lewis, 1978; Struhl, 1981). For example, mutations in *Pc* lead to the development of embryos with thoracic and abdominal segments transformed into the more posterior eight abdominal segments (Lewis, 1978). Likewise, mutations in *E(z)* lead to similar mutant phenotypes in *Drosophila* (Jones and Gelbart, 1990). These mutations are typically embryonic lethal, but clonal analyses and hypomorphic mutants demonstrate that these genes act throughout post-embryonic development to maintain proper Hox gene expression in imaginal discs. Mutations in PcGs typically lead to ectopic sex combs on meso- and metathoracic legs, indicating that these legs transform into a prothoracic leg identity (Jones and Gelbart, 1990). This transformation is accompanied by ectopic expression of *Sex combs reduced* in meso- and metathoracic leg imaginal discs (Glicksman and Brower, 1988; Jones and Gelbart, 1990). In addition, mesothoracic wing discs express ectopic Ultrabithorax (Ubx) and consequently, forewings partially acquire a haltere identity (Cabrera et al., 1985).

Recent studies in the hemimetabolous cricket *Gryllus bimaculatus* embryos demonstrate similar Hox maintenance roles: removal of E(z) and Su(z)12 results in shifts in the anterior limit of Hox genes, indicating that PcGs play critical roles in repressing the posterior Hox genes in anterior portions of the developing embryo (Matsuoka et al., 2015). Interestingly, while PcGs appear to maintain the anterior expression boundaries of all Hox genes that are initially established by gap genes in *Drosophila*, the posterior Hox genes expression boundaries are established by PcGs themselves in *Gryllus*. Thus, the roles of PcGs in establishing and maintaining Hox gene expression appear to have undergone changes within the insects (Matsuoka et al., 2015).

In addition to regulating Hox genes, recent studies have demonstrated that PcG proteins regulate many additional processes, including stem cell biology, cancer development, and regeneration (Aloia et al., 2013; Sauvageau and Sauvageau, 2010; Schuettengruber et al., 2017). Limb regeneration in vertebrates and invertebrates occurs in three major steps: wound healing, blastema formation, and re-differentiation (Endo et al., 2004). After amputation of a limb, epithelial cells migrate to the amputation site and form the wound epidermis, a transient epithelium crucial for subsequent outgrowth (Brockes, 1997; Endo et al., 2004; Mitten et al., 2012). The blastema is formed when either pre-existing stem cells or de-differentiated cells underneath the epithelium begin to proliferate (Echeverri and Tanaka, 2002; Konstantinides and Averof, 2014; Kragl et al., 2009; Sandoval-Guzman et al., 2014). Subsequently, various tissue types are re-patterned to recreate a limb (Brockes, 1997; Hamada et al., 2015; Konstantinides and Averof, 2014). The regeneration process depends largely on the cells' abilities to undergo significant changes in proliferative activity after the activation of specific differentiation programs (Rouhana and Tasaki, 2016). These changes are coupled with the activation of normally silent chromatin (Stewart et al., 2009), suggesting that epigenetic histone regulators are used to temporarily maintain cells in a dedifferentiated state. Furthermore, studies in the frog *Xenopus laevis* have demonstrated that histone modifications might be important for maintaining cell identity during limb regeneration (Hayashi et al., 2015). In zebrafish, the histone demethylase KDM6 is necessary for fin regeneration (Stewart et al., 2009). In larval zebrafish, the homolog of E(z), EZH2, is necessary for caudal fin regeneration: caudal fins do not regenerate properly in both larval zebrafish treated with a chemical EZH2 inhibitor and *EZH2* mutant larvae (Dupret et al., 2017).

A recent study in crickets showed that the knockdown of *E(z)* leads to the addition of an extra tibial segment during leg regeneration through the expansion of the expression domain of the medial leg specifier gene *dachshund* (Hamada et al., 2015). In contrast, knockdown of H3K27 demethylase, *Ubiquitously transcribed tetratricopeptide repeat gene on the X chromosome* (*Utx*), in crickets leads to altered expression of *Egfr* and causes defects in tarsal joint formation (Hamada et al., 2015). Thus, both of these genes are necessary for proper re-patterning of amputated legs but are not necessary for de-differentiation, blastema formation and blastema differentiation (Hamada et al., 2015). In *Drosophila* imaginal discs, fragmentation of prothoracic legs leads to reduced PcG gene expression, facilitating leg-to-wing transdetermination of the imaginal discs (Lee et al., 2005).

In this study, we sought to determine the roles of PcG proteins during metamorphosis and limb regeneration in the red flour beetle *Tribolium castaneum*, a holometabolous insect. Unlike *Drosophila*, *Tribolium* undergoes a more typical mode of development where the larval epidermal cells are retained and contribute to the adult epidermis. Thus, this species is an interesting model to explore the role of PcG proteins during post-embryonic development. Specifically, while Hox genes are necessary to specify segmental identity during metamorphosis in the *Tribolium* (Tomoyasu et al., 2005; Smith and Jockusch, 2014), whether or not PcG proteins play a role in regulating the expression of Hox genes remains unknown. In addition, *Tribolium* larval legs are amenable to regeneration studies as RNAi works well in this species (Shah et al., 2011). *Tribolium* provides an interesting contrast to the crickets because larval legs comprise of partially differentiated precursor cells, not differentiated cells as observed in cricket nymphs (Truman and Riddiford, 2002; Villarreal et al., 2015).

Specifically, we chose to study the post-embryonic functions of Pc and E(z) in *Tribolium*. Pc was one of the first PcG proteins discovered in *Drosophila* (Lewis, 1947, 1978) that plays a critical role in the canonical PRC1 (Wang et al., 2004b). E(z) has been shown to play a role during

regeneration in a number of species and is a critical member of PRC2 (Cao et al., 2002; Cao and Zhang, 2004; Czermin et al., 2002). Both of these proteins have been demonstrated to bind to the promoter of *Ubx* in wing imaginal discs (Wang et al., 2004b). We show that knockdowns of *Pc* or *E(z)* during metamorphosis lead to the development of adults with distinct developmental abnormalities that include, but are not limited to, homeotic transformations. In addition, *Pc* and *E(z)* are required for proper limb regeneration, and their removal results in the absence of re-differentiation.

2. Materials and methods

2.1. Beetle husbandry

Tribolium castaneum GA-1 strain was acquired from Dr. Richard Beeman (USDA ARS Biological Research Unit, Grain Marketing & Production Research Center, Manhattan, Kansas). The beetles were raised on organic wheat flour containing 5% nutritional yeast and were kept in a 29 °C incubator with ~50% relative humidity in plastic containers. Fumagillin (0.5%), an antibiotic, was added to the diet halfway through the project when the colony experienced a sudden decline.

2.2. mRNA isolation and cDNA synthesis

Larvae were dissected in 1X-phosphate-buffered saline (PBS; 0.02 M phosphate, 0.15 M NaCl, 0.0038 M NaH_2PO_4, 0.012 M Na_2HPO_4; pH 7.4) to take out the gut and the fat body. The remaining tissue was homogenized in Trizol (Invitrogen), and RNA was then extracted using chloroform, treated with DNase (Promega), and precipitated in isopropyl alcohol. cDNA was synthesized from 1 μg of total RNA via the cDNA synthesis kit (Fermentas) following the manufacturer's instructions.

2.3. Cloning and double-stranded RNA (dsRNA) synthesis

Sequences of *Pc* and *E(z)* were acquired from sequences deposited in GenBank (*Pc* GenBank accession number XM_008199399; *E(z)* GenBank accession number XM_001811600), and fragments were amplified using the primers listed (Supplemental Table 1). The amplified cDNA product was isolated and cloned into a TOPO TA vector (Invitrogen). After plasmid identity was confirmed by sequencing, plasmid DNA was linearized through restriction digestion. The strands of dsRNA were synthesized with T3 and T7 MEGAscript Kits (Ambion) using the manufacturer's instructions. Single-stranded RNAs (ssRNAs) were combined and annealed to create dsRNA (Hughes and Kaufman, 2000). For the control, dsRNA targeting bacterial *ampicillin resistance* (*amp^r*) gene was used. The annealed product was analyzed via gel electrophoresis to confirm annealing, then was stored at −80 °C until use. The final concentrations of the dsRNA were 2 μg/μL for all genes.

2.4. Double-stranded RNA injection

For regeneration studies, day zero sixth instar larvae (seventh or eighth instar is considered the final instar within our colony) were injected with approximately 0.5 μg (0.25 μL) of dsRNA between the first and second abdominal segments of their dorsal side with a pulled 10-μL glass capillary needle connected to a syringe. *amp^r* dsRNA was injected into larvae as the control. These dsRNA-treated larvae were maintained at normal conditions (29 °C in whole wheat flour containing 5% yeast) until their appendages were ablated two days later. Ablation was delayed to ensure that the RNAi-mediated knockdown was fully effective prior to appendage cuts (Shah et al., 2011). For studies on the roles of *E(z)* and *Pc* during metamorphosis, seventh or eighth instar larvae were injected with 1 μg (0.5 μL) of dsRNA on day zero.

2.5. Knockdown verification

Three day zero sixth instar larvae were injected with 0.25 μl of each of the dsRNA used in this study. On day zero of the seventh instar, larvae were pooled in Trizol, and the isolated RNA was converted to cDNA as described above. Semi-quantitative PCR was performed to determine the knockdown of the targeted genes. Primers used are listed in Supplemental Table 1. The cycle number used were as follows: 32 cycles for *rp49*, 40 cycles for *Pc*, and 38 cycles for *E(z)*.

2.6. Leg ablations

Two days after dsRNA injections, larval mid- and hindlimbs were either cut at the coxa or the femur on one side of the larva. The larvae were anesthetized on ice and were placed on a slide covered with double-sided tape with the ventral side up. Under a dissecting microscope, their legs were ablated using fine microscissors. To ablate antennae, antennae of anesthetized larvae were cut near the boundary of the antennifer and the scapus using a fine blade.

2.7. Quantitative PCR

To examine the expression of *Ubx* in the second thoracic segment (T2) and the third thoracic segment (T3), day 0 seventh instar larvae were injected with 0.5 μL dsRNA. Once they reached the prepupal stage, T2 segments and T3 segments were isolated by separating the segments using a microscissor. Segments from three prepupae were pooled to create one biological replicate, and a total of three biological replicates were generated. These samples were homogenized in Trizol, and their RNA was purified and converted to cDNA as described above. SsoAdvanced Universal SYBR Green Supermix (Bio-Rad) was used to run the qPCR. Three technical replicates were run for each biological replicate and *rp49* was used as an internal control. Primers used are listed in Supplemental Table 1. A standard curve was generated and used to analyze the data.

3. Results

3.1. Knockdown verification

RNA from day zero seventh instar larvae injected with *amp^r*, *Pc* or *E(z)* dsRNA as day zero sixth instar was collected to verify proper knockdown of the targeted genes. We found that relative to *amp^r* dsRNA injected control larvae, *Pc* and *E(z)* expression was reduced in larvae injected with *Pc* and *E(z)* dsRNA, respectively (Supplemental Fig. 1). Thus, *Pc* and *E(z)* were successfully silenced in response to dsRNA injection.

3.2. Pc RNAi leads to disrupted eye development and homeotic transformation of appendages

To determine the role of *Pc* during *Tribolium* metamorphosis, approximately 1 μg of *Pc* dsRNA was injected into day zero seventh or eighth instar larvae. The majority of larvae injected metamorphosed without undergoing an extra larval-larval molt (n = 16/18; Table 1), similar to the *amp^r* dsRNA-injected larvae (n = 10/10). Unlike *amp^r* dsRNA-injected pupae (Fig. 1B', C', open arrows), the *Pc* knockdown pupal head was misshapen with a narrower posterior margin of the head relative to the anterior end (Fig. 1D', E', open arrows). In addition, while the head of *amp^r* dsRNA-injected pupae underwent rotation such that the head was ventrally located (Fig. 1B', C', open arrows), the head of *Pc* knockdown pupa failed to rotate and remained in the anterior-facing position (Fig. 1D', E', open arrows). The compound eyes failed to develop (Fig. 1F'', black arrowhead), and the legs were improperly folded (Fig. 1F'). In *amp^r* dsRNA-injected animals, wings cover the legs on the ventral side, but *Pc* knockdown pupae had smaller wings that were positioned laterally (Fig. 1C, F', dotted lines). The prothorax was oval-

Table 1
Effects of *Pc* and *E(z)* knockdown on metamorphosis. Larvae were injected on day 0 seventh or eighth larval instar.

Targeted gene	Total nr	Underwent larval-larval molt	Died as larva	Died as prepupa	Died as pupa	Died as pharate adult	Survived to normal adult
amp^r	10	0	0	0	0	0	10
Pc	18	2	1	0	3	13	1
E(z)	17	4	3	3	1	9	1

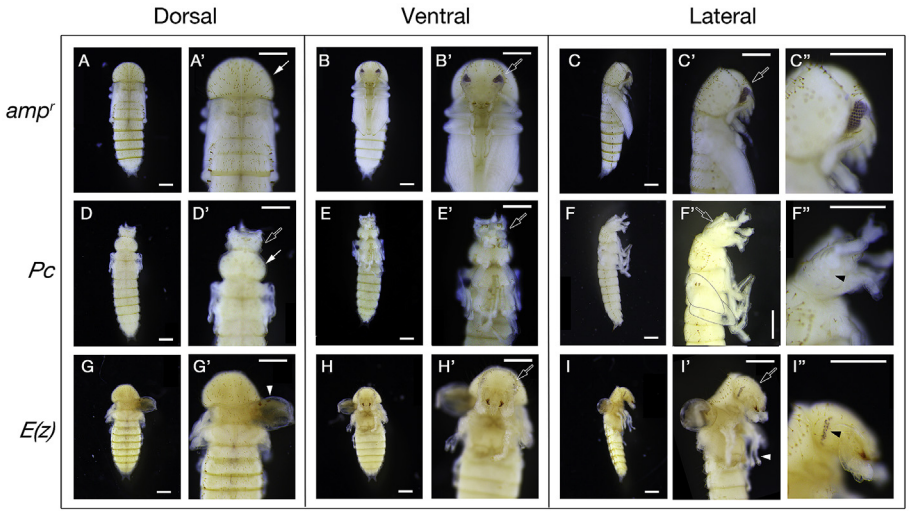

Fig. 1. *Pc* and *E(z)* knockdowns disrupt proper appendage and eye development in *Tribolium* pupae. Effects of (A–C) *amp^r*, (D–F) *Pc* and (G–I) *E(z)* knockdowns on pupal morphology. Seventh instar larvae were injected with approximately 1 μg (0.5 μL) of dsRNA on day zero. (A, D, G) Dorsal views, (B, E, H) ventral views, and (C, F, I) lateral views of pupae are shown. (A', B', D', E', G', H') Head and prothorax morphologies of pupae. *Pc* knockdown pupae have misshapen pronota and fail to rotate their heads. Open arrows point to heads, and white arrows point to pronota. (C', F', I') Wing and leg morphology (white arrowheads). *Pc* and *E(z)* knockdown pupae have shortened wings and improperly folded appendages. Wings in C and F' are outlined with black dotted lines. (C'', F'', I'') Compound eye development. *Pc* knockdown pupae failed to develop compound eyes (F'', black arrowhead), whereas *E(z)* knockdown pupae had disrupted compound eye development (I'', black arrowhead). Each scale bar represents 0.5 mm.

shaped and reduced in size relative to *amp^r* dsRNA-injected adults (Fig. 1A', D', white arrows).

While a few pupae were arrested at the pupal stage, the majority of *Pc* knockdown survived to the pharate adult stage and died (n = 13/18; Table 1). These pharate adults had misshapen heads with dramatically reduced sclerotization (Fig. 2G, G', white arrowheads; Fig. 3E, E'). In *amp^r* dsRNA-injected animals, the head capsule forms a single integrated unit (Fig. A, A'). In contrast, the head of *Pc* knockdown adults had several sclerotized cuticular patches. On the ventral side, two large patches of sclerotized cuticle were observed (Fig. 3E, dotted lines). On the dorsal side, three large patches of sclerotized cuticle were observed; two were located between the eyes and the antennae, and one was located between the antennae (Fig. 3E', dotted lines). The latter had prominent bristles, suggesting that the structure was a labrum although it was smaller than and morphologically distinct from the labrum of the *amp^r* dsRNA-injected adult (Fig. 3D, H). The compound eyes failed to develop properly (Fig. 2I, open arrow) and were much reduced in size relative to those of *amp^r* dsRNA-injected animals (Fig. 2D). In addition, the abdomens of *Pc* knockdown adults were elongated and stretched out, suggesting that the compaction of the body that occurs during metamorphosis failed to take place (Fig. 2E, J, J'). Moreover, the sternal plates were narrower and appeared to have undergone partial homeotic transformation as notches that appear in the more posterior abdominal sternites of wildtype adults (Fig. 2E, arrowheads) were present on all abdominal sternites of the more severely affected *Pc* knockdown adults (Fig. 2J', black arrowheads). In particular, an additional sternite-like structure developed at the posterior end of some adults, indicating that the genitalia-bearing segment had undergone anterior transformation (Supplemental Fig. 2; Fig. 2J', black

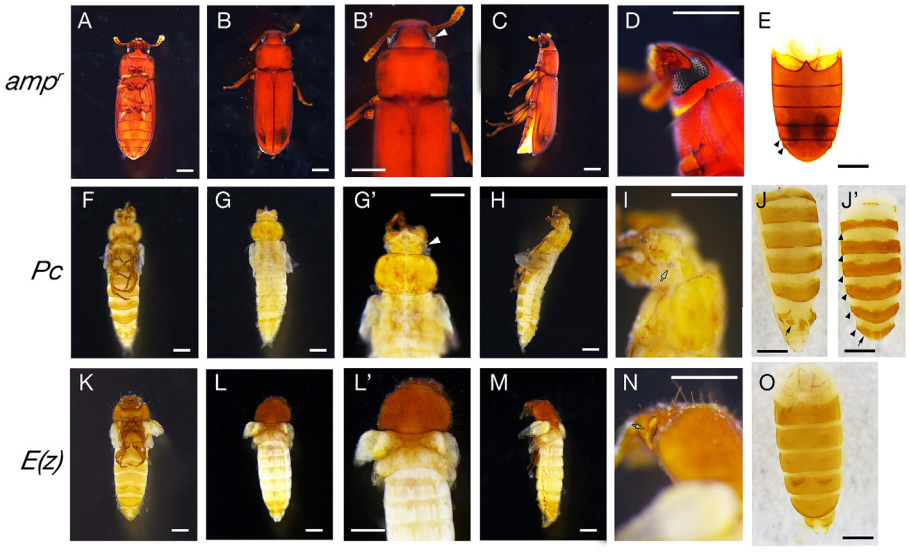

Fig. 2. *Pc* and *E(z)* knockdown *Tribolium* adults exhibit extensive head, appendage and eye defects. Effects of (A–E) *amp^r*, (F–J) *Pc* and (K–O) *E(z)* knockdowns on adult morphology. (A, E, F, J, K, O) Ventral views, (B, G, L) dorsal views and (C, H, M) lateral views of dsRNA-injected animals. White arrowheads point to heads. (D, I, N) Head morphology of dsRNA-injected adults showing disrupted eye development in *Pc* and *E(z)* knockdown adults. Open arrows indicate disrupted eyes. (E, J, O) Isolated abdomens of dsRNA-injected adults. All abdominal sternites of *Pc* knockdown adults had notches (J', arrowheads), which normally develop on the more posterior abdominal segments (E, arrowheads). In addition, several adults (J') developed an extra abdominal sternite-like structure at the posterior end, whereas others (J) had increased sclertotization but not to the extent that a complete sternite-like structure formed (black arrows). Each scale bar represents 0.5 mm.

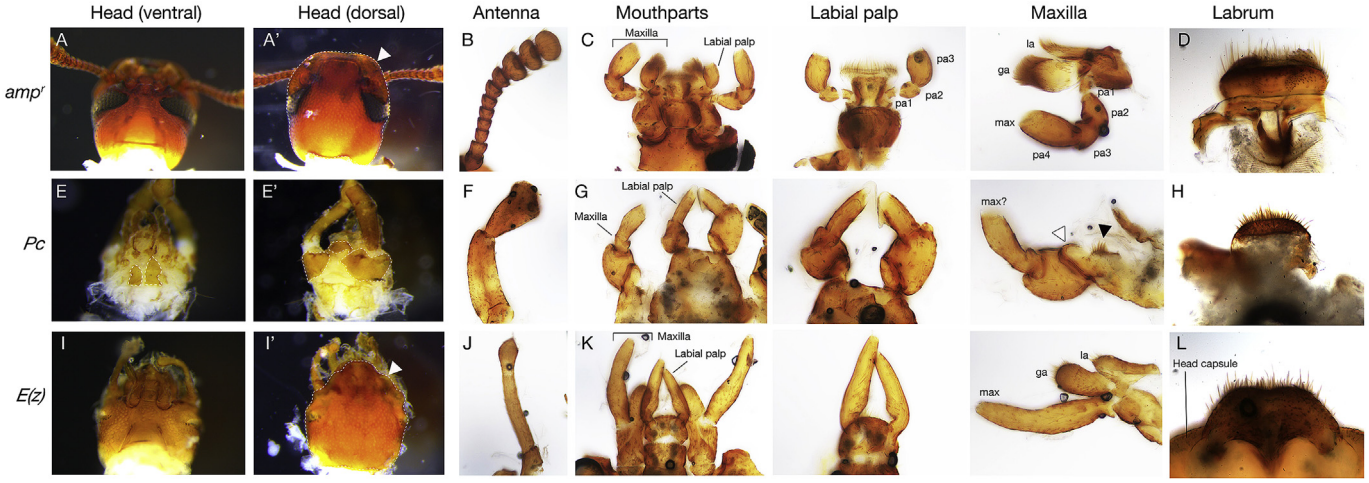

Fig. 3. *Pc* and *E(z)* knockdown head appendages exhibit homeotic transformations and patterning defects in adult *Tribolium*. Effects of (A–D) *amp*^{r}, (E–H) *Pc* and (I–L) *E(z)* knockdowns are shown. (A, E, I) Ventral view of the head. (A', E', I') Dorsal view of the head. White arrowheads point to anterior portion of the head capsule, which was misshapen in the *E(z)* knockdown adult (I'). Dotted lines outline the dorsal head capsule or sclerotization. (B, F, J) Antennae of *amp*^{r} (B), *Pc* (F) and *E(z)* (J) dsRNA-injected adults. (C, G, K) Labial palps and maxillae of *amp*^{r} (C), *Pc* (G) and *E(z)* (K) dsRNA-injected adults. (Left) Labial palps and maxillae before dissections. (Center) Labial palps of dsRNA-injected animals. (Right) Maxillae of knockdown animals. Pa = palpomeres; max = maxillary palp; ga = galea; la = lacinia. Black arrowhead points to a possible remnant of the galea. Open arrowhead points to the trochanter-like structure. (D, H, L) Labrum of *amp*^{r} dsRNA-injected adults. (H) Labrum-like structure isolated from *Pc* knockdown adult head. (L) Close-up of the anterior end of the head capsule of *E(z)* knockdown adults from the ventral side. A labrum-like structure was fused to the head capsule.

arrow; n = 5/10). Other adults also had increased sclerotization in the sixth abdominal segment although not to the extent that a sternite-like structure was formed (Fig. 2J, black arrow; n = 4/10). Whether the differences arise from differences in the sex of the adults or in the severity of the knockdown was not clear.

The head appendages were dramatically altered in *Pc* knockdown pharate adults (Fig. 3). Whereas normal *amp*^{r} dsRNA-injected adults have 11 antennal segments (Fig. 3B), the *Pc* knockdown antennae consisted of two large segments that resembled leg segments (Fig. 3F). In particular, the proximal segment had a superficial resemblance to the femur. In addition, the labial palps were enlarged and the relative sizes of the segments were altered: the distal-most palpomere 3 in *amp*^{r} dsRNA-injected adults is the largest labial segment (Fig. 3C, center, pa3); in contrast, in *Pc* knockdown adults, the basal segment in the labial palp was enlarged with a superficial femur-like appearance (Fig. 3G, center). The maxillary palps of *Pc* knockdown adults were also dramatically altered such that the basal presumptive palpomere segment was enlarged relative to the distal presumptive palpomere segment (Fig. 3G, right), unlike in *amp*^{r} dsRNA-injected adults whose distal-most palpomere was the largest of the four (Fig. 3C, right). The enlarged segment of *Pc*-RNAi maxillary palp resembled a femur with a trochanter-like structure (Fig. 3G, right). In addition, the galea and the lacinia were almost absent in *Pc* knockdown adults. In *Pc* knockdown adults, therefore, the maxilla appeared to have transformed from a branched appendage to a non-branched appendage. Taken together, in the absence of *Pc*, both the maxilla and the labial palps resembled each other and assumed a more leg-like morphology.

In normal *amp*^{r} dsRNA-injected *Tribolium* adults, the forelegs and midlegs have five tarsal segments, whereas the hindlegs have four tarsal segments and are longer than the fore- and midlegs (Figs. 4A-A'' and 5B, C). All three pairs of legs in *Pc* knockdown adults had four tarsomeres and were similar in size (Figs. 4B-B'' and 5B, C). This suggests that the foreleg and midleg may have undergone homeotic transformation to adopt a hindleg identity. In support of this idea, none of the 11 pharate adults examined had foreleg-specific pads that are found in males (Fig. 4A, white arrowhead). Although we were unable to properly sex the adults, at least a few of these should have been males.

The fore- and hindwings of *Tribolium* adults are morphologically distinct: the forewings are characterized by the development of

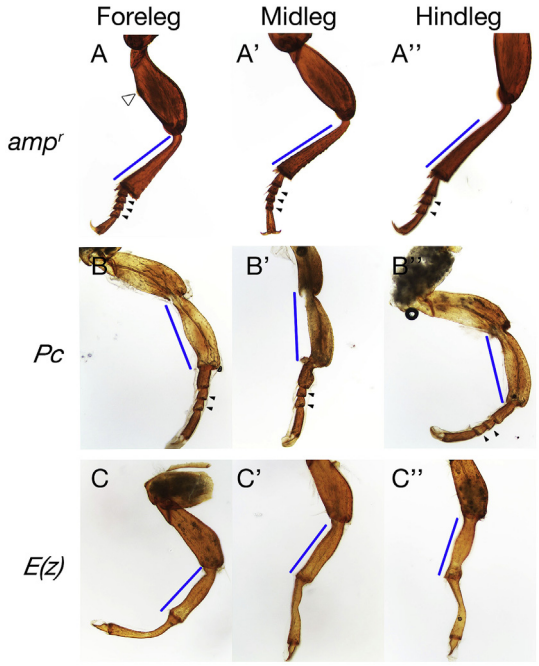

Fig. 4. *Pc* and *E(z)* knockdown *Tribolium* adult legs exhibit homeotic transformations and patterning defects. Effects of (A) *amp*^{r}, (B) *Pc* and (C) *E(z)* knockdowns on adult leg morphology. (A, B, C) Foreleg, (A', B', C') midleg and (A'', B'', C'') hindleg of knockdown adults. The medial tarsal segments are indicated by arrowheads. Blue lines represent the length of the foreleg tibia for each of the knockdown animals. Open arrowhead represents the male-specific pad on the foreleg of *amp*^{r} dsRNA-injected animals.

sclerotized elytra whereas the hindwings are membranous wings (Fig. 6A). In addition, a sclerotized structure called the scutellum forms at the base of the sclerotized elytra (Fig. 6A, black arrow). In *Pc* knockdown adults, instead of a pair of elytra, a pair of small membranous wings was observed in the mesothoracic segment, and the scutellum was missing (Fig. 6B), indicating that the forewing had undergone homeotic

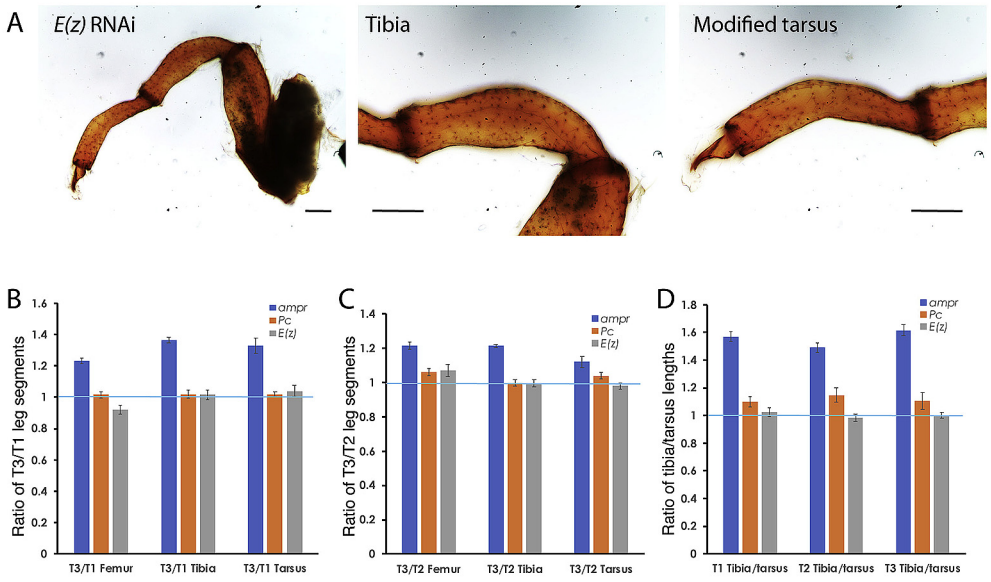

Fig. 5. *Pc* and *E(z)* knockdowns lead to uniform leg segment lengths across the three thoracic segments of *Tribolium* adults. Relative sizes of the appendage segments in *amp*^{r}, *Pc* and *E(z)* dsRNA-injected adults are shown. (A) *E(z)* knockdown leg showing the disrupted tarsal segment. (Middle) Close-up of the tibia. (Right) Close-up of the modified tarsus. Scale bars represent 0.1 mm. (B) Comparison of T1 and T3 leg segment sizes. The T3/T1 leg segment ratios are plotted. (C) Comparison of T2 and T3 leg segment sizes. The T3/T2 leg segment ratios are plotted. (D) Comparison of tibial and tarsal leg segment sizes. Tibia/tarsus ratios are plotted. Each bar represents an average of 6–7 measurements. Error bars represent standard error. Blue line represents a ratio of 1, indicating identical lengths.

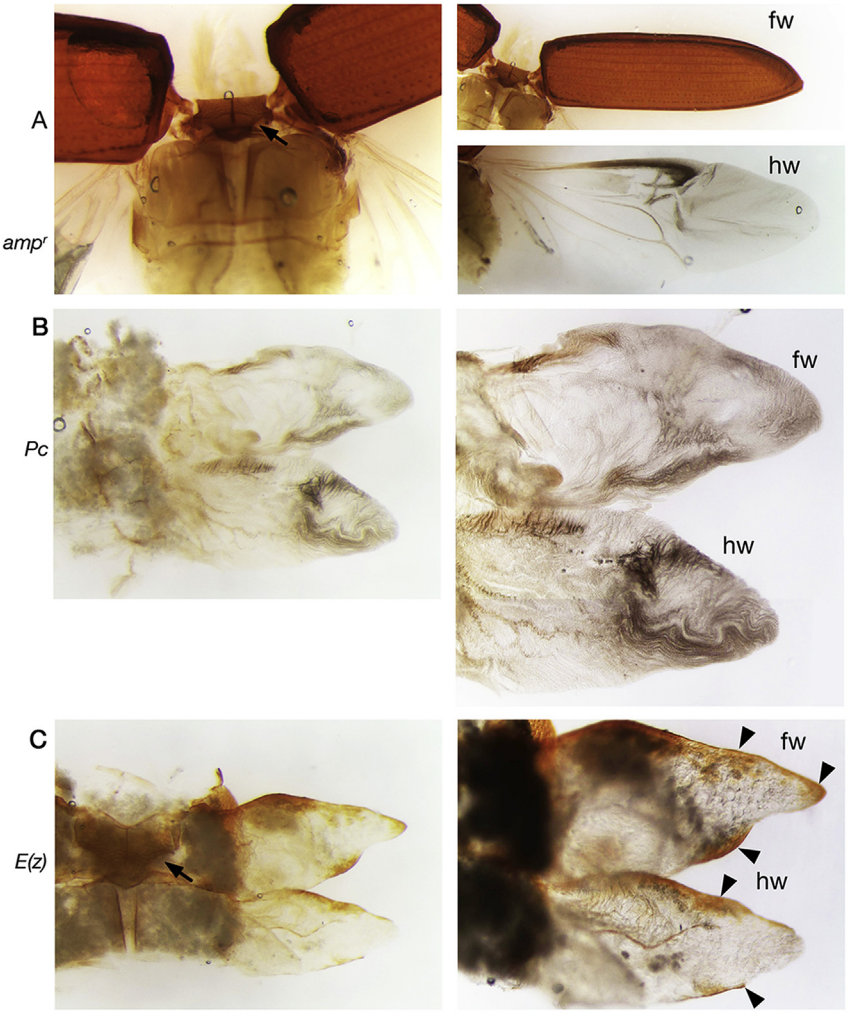

Fig. 6. *Pc* and *E(z)* knockdown leads to homeotic transformations of wings in *Tribolium* adults. Effects of (A) *amp*^{r}, (B) *Pc* and (C) *E(z)* dsRNA-injection on adult wing morphology. Left panels show the wings and the dorsal segment. Arrows point to the scutellum of *amp*^{r} and *E(z)* dsRNA-injected adults; the scutellum did not appear to develop in the *Pc* knockdown animal. (B, C, right) Wings imaged under a compound microscope. Sclerotized areas are marked with arrowheads.

transformation to adopt a hindwing-like identity. We note that although the wings failed to extend, we did not see sclerotization in either of the wings even when the rest of the body was sclerotized.

To characterize the nature of this homeotic transformation, we examined the expression of the Hox gene *Ubx*, which specifies the third thoracic segment (T3) identity, in both the second thoracic segment (T2) and T3 in *amp*^{r} and *Pc* knockdown prepupae. We found that *Ubx* is significantly upregulated in T2 of *Pc* knockdown prepupae compared to *amp*^{r} dsRNA-injected prepupae (Fig. 7A; $p < 0.0001$, Student's t-test). In contrast, no significant differences were observed between the *Ubx* expression in T3 of *amp*^{r} and *Pc* knockdown prepupae (Fig. 7B; $p = 0.09$, Student's t-test). Taken together, these results indicate that in *Pc* knockdown prepupae, *Ubx* is misexpessed in T2, transforming T2 into T3 during metamorphosis.

3.3. *E(z) RNAi leads to partial homeotic transformation and tarsus-to-tibia transformations*

To determine the role of *E(z)* during *Tribolium* metamorphosis, approximately 1 μg of *E(z)* dsRNA was injected into day zero seventh or eighth instar larvae. The majority of larvae metamorphosed without undergoing an extra larval-larval molt ($n = 13/17$; Table 1). The wings of *E(z)* knockdown pupa were reduced in size and failed to fold ventrally over the legs (Fig. 1G', white arrowhead). The appendages also failed to fold properly (Fig. 1I', white arrowhead) although the head rotation was normal (Fig. 1H', I', open arrows). The compound eyes began to develop although they did not complete their development and were disorganized (Fig. 1I'', black arrowhead).

The majority of *E(z)* knockdown animals that pupated arrested in the pharate adult stage ($n = 9/11$; Table 1). While the compound eyes were more developed than *Pc* knockdown animals, they were reduced in size

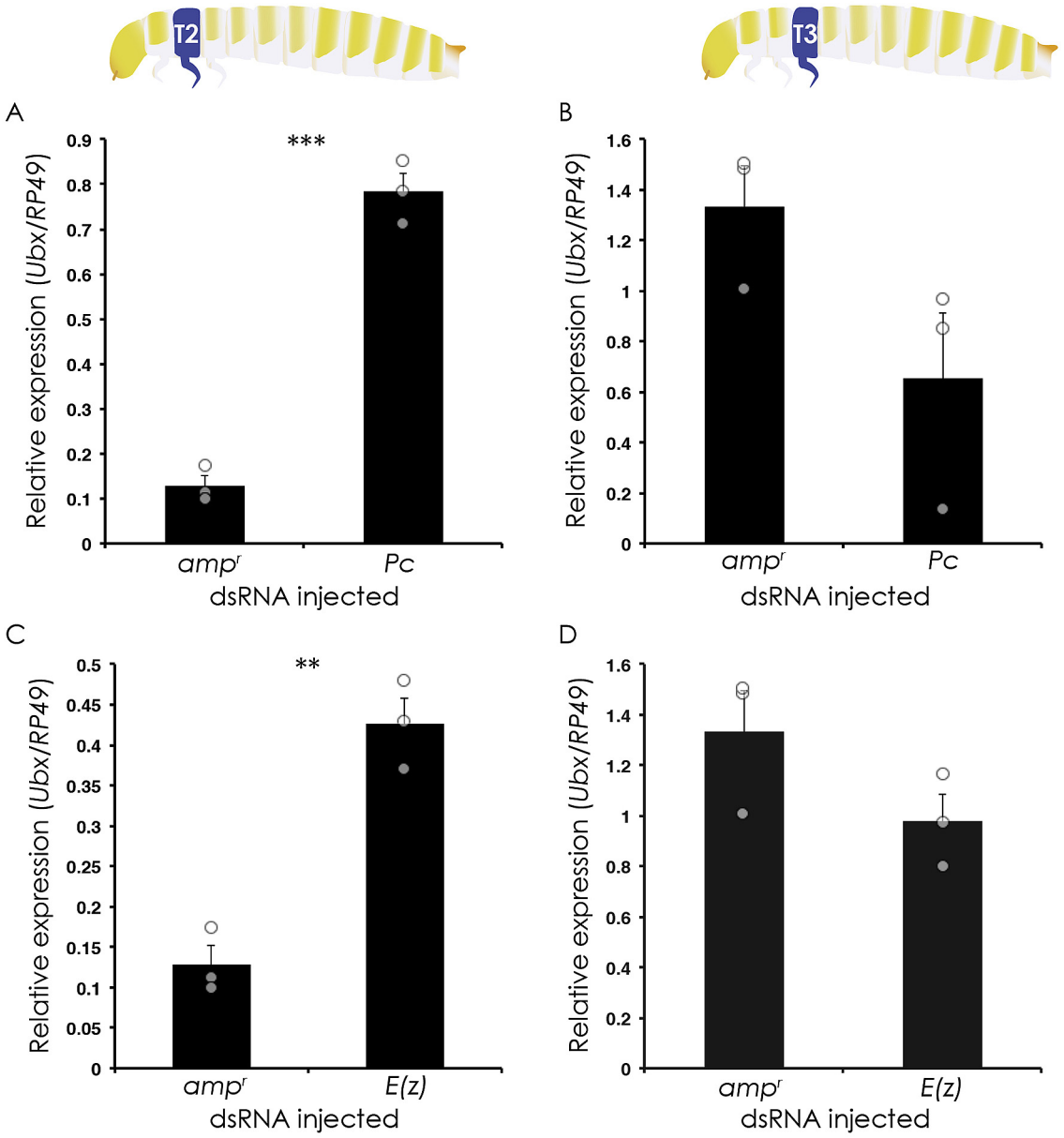

Fig. 7. *Ubx* expression is upregulated in T2 after *Pc* (A, B) or *E(z)* (C, D) knockdown. (A, B) Average expression of *Ubx* in T2 (A) and T3 segments (B) of *Pc* or *amp*^{r} dsRNA-injected prepupae. (C, D) Average expression of *Ubx* in T2 (C) and T3 segments (D) of *E(z)* or *amp*^{r} dsRNA-injected prepupae. Quantitative PCR was used to measure the expression of *Ubx*. Expression was normalized using *rp49* as an internal control. Averages represent means of three biological replicates. Error bars represent standard error. Individual values are represented by the circles. ** denotes $p < 0.005$; *** denotes $p < 0.0001$. Expression in T3 is not significantly different.

(Fig. 2N, open arrow). The head capsule developed although the anterior portion was misshapen (Fig. 3I', white arrowhead). The anterior portion of the head capsule had prominent bristles, and given the lack of a distinct labrum, we suspect that the labrum was fused to the anterior end of the head capsule (Fig. 3L). The abdomen of *E(z)* knockdown adults did not appear to undergo the dramatic homeotic transformations observed in *Pc* knockdown adults (Fig. 2O). All of the head appendages lacked segmentation and were dramatically elongated (Fig. 3I, J, K). While the proximalmost segment of the antenna was visible, the rest of the segments failed to form, and the antenna developed as a slender rod (Fig. 3J). Similarly, the labial palp and the maxilla also lacked visible segmentation (Fig. 3K). Unlike the *Pc* knockdown maxilla, the galea and the lacinia developed normally although their morphology was altered compared to the galea and the lacinia observed in the *amp^r* dsRNA-injected animals (Fig. 3C).

The fore-, mid- and hindlegs all had dramatically altered tarsal segments and formed a single leg segment that superficially resembled a tibia (Figs. 4C-C", 5A). Moreover, the length of this altered tarsus was similar to the tibia (Fig. 5D). In addition, the three pairs of legs resembled each other and were similar in length (Fig. 5B and C). Thus, like *Pc* knockdown animals, the legs on the three thoracic segments were indistinguishable from each other. None of the nine pharate adults examined had any patches characteristic of male forelegs, suggesting that all the legs had transformed into a T2 or T3 identity.

Lastly, the fore- and hindwings of *E(z)* knockdown pharate adults resembled each other, similar to *Pc* knockdown animals (Fig. 6C). In more severely affected *E(z)* knockdown animals, the forewing did not exhibit any sclerotization except at the margins (Fig. 6C). Similarly, the hindwings also had ectopic sclerotization around the margins. Thus, the fore- and hindwings both comprised of sclerotized and unsclerotized regions, leading us to speculate that both wings in *E(z)* knockdown adults adopt an intermediate T2/T3 identity. The wings were also reduced in size, suggesting that E(z) might play a role in the proliferation of wing imaginal cells.

To clarify the nature of transformations, we examined whether *Ubx* might also be misexpressed in T2 of *E(z)* knockdown prepupae. Similar to *Pc* knockdown larvae, *E(z)* knockdown led to significant upregulation of *Ubx* in T2 compared to *amp^r* dsRNA-injected (Fig. 7C; $p < 0.005$, Student's t-test). No significant difference in *Ubx* expression was observed between T3 of *E(z)* and *amp^r* dsRNA-injected prepupae (Fig. 7D; $p = 0.14$, Student's t-test). Thus, in the absence of *E(z),* T2 appendages likely undergo partial transformation to T3-like appendages.

Taken together, these results indicate that in *Tribolium*, E(z) and Pc play critical roles in specifying the segmental identities of appendages during metamorphosis. Moreover, both Pc and E(z) play additional roles in patterning imaginal cell-derived structures: both genes are necessary for adult compound eye development and growth of wings, and E(z) is necessary for proper patterning and segmentation of the tarsus and head appendages.

3.4. Knockdown of Pc expression inhibits leg regeneration after ablation at the coxa

To elucidate how *Pc* silencing affects *Tribolium* regeneration, dsRNA was injected into day zero sixth instar larvae. Mid- and hindlegs on one side of these larvae were cut two days later at the coxa, and regeneration of the ablated appendages was recorded after every molt (Table 2). In *amp^r* dsRNA-injected control *Tribolium* larvae, wound healing and formation of blastema-like structures were observed after the first larval molt. After the second larval molt, segments were reformed (Fig. 8A). Pupae that developed from *amp^r* dsRNA-injected larvae after one and two larval molts exhibited regenerated limbs as previously described (not shown; Shah et al. (2011)).

All *Pc* knockdown *Tribolium* larvae showed wound healing at the leg ablation sites similar to *amp^r* dsRNA-injected controls after one larval molt. These larvae also exhibited blastema-like structures at the ablation sites. After the second molt, approximately half of the surviving *Pc* dsRNA-injected larvae showed no further regeneration (Fig. 8B), while the rest exhibited partial regeneration in at least one leg (Table 2; Fig. 8C). One larva that pupated after one molt exhibited regeneration whereas another larva that pupated after two molts exhibited no regeneration (Fig. 8E). These results indicate that *Pc* is required for regeneration in *Tribolium* although the effect is variable, possibly due to incomplete knockdown of *Pc* or redundant functions of additional regulators.

3.5. E(z) is essential for the regeneration of legs after ablation at the coxa

To determine how *E(z)* knockdown affects regeneration, *E(z)* dsRNA was injected into day zero sixth instar larvae ($n = 23$). Mid- and hindlegs on one side of these larvae were cut two days later at the coxa, and regeneration of the ablated appendages was recorded after every molt. Treated larvae were observed during their subsequent life stages. All *E(z)* knockdown larvae showed wound healing at the leg ablation sites similar to *amp^r* dsRNA-injected controls and *Pc* dsRNA-injected larvae after one larval molt. These animals also exhibited blastema-like structures at the ablation sites. Nine out of 23 larvae died after the first molt. None of the *E(z)* dsRNA-injected larvae that underwent a second larval-larval molt regenerated their legs ($n = 12$, Fig. 8D; Table 2). The pupae that formed after one or two larval molts also exhibited no regeneration (Table 2). These results indicate that *E(z)* is essential for leg regeneration in *Tribolium*.

A previous study demonstrated that *Gryllus* leg regeneration does not require E(z) for blastema differentiation but is necessary for the proper re-patterning of the leg: knockdown of *E(z)* leads to the formation of an extra tibial segment (Hamada et al., 2015). The *Gryllus* legs, however, were amputated at the tibia or the femur, not at the coxa as in our study. To determine whether amputation position might impact regeneration, we injected sixth instar larvae with *Pc, E(z)* or *amp^r* dsRNA and amputated the legs at two different segments two days later: the midleg was

Table 2
Effects of *Pc* and *E(z)* knockdown on leg regeneration. Larvae were injected and ablated during the sixth larval instar.

Targeted gene	Total nr	Larvae after 1 molts			Larvae after 2 molts		
		Nr with regenerated legs	Nr without regenerated legs	Died before pupation after 1 molt	Nr with regenerated legs	Nr without regenerated legs	Died before pupation after 2 or 3 molts
amp^r	7	0	7	0	5	0	0
Pc	19	0	19	2	9	7	15
E(z)	23	0	23	9	0	12	11

Targeted gene	**Total nr pupated**	**Pupa after 1 molt**		**Pupa after 2 molt**	
		Nr with leg regeneration	Nr without leg regeneration	Nr with leg regeneration	Nr without leg regeneration
amp^r	7	2	0	5	0
Pc	2	1	0	0	1
E(z)	3	0	2	0	1

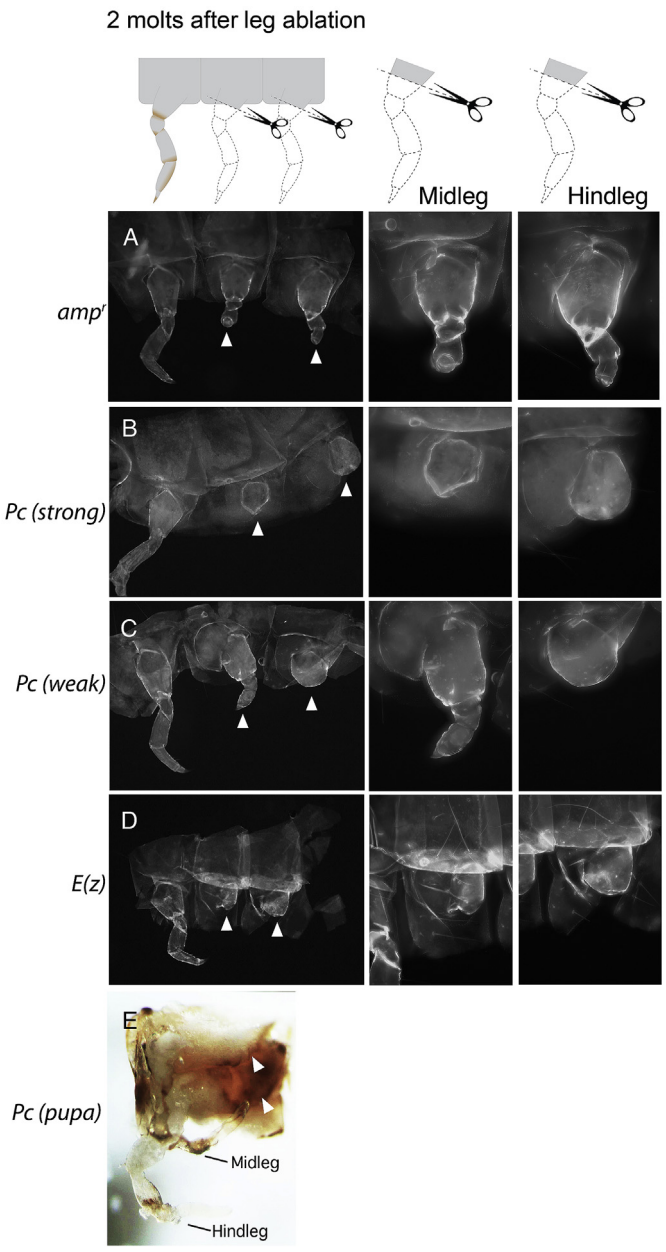

Fig. 8. *Pc* and *E(z)* are necessary for proper larval leg regeneration post coxal ablation in *Tribolium*. Effects of (A) *amp*^{r}, (B, C, E) *Pc* and (D) *E(z)* dsRNA-injection on *Tribolium* leg regeneration after two larval molts. Day zero sixth instar larvae were injected with 2 μg/μL *amp*^{r}, *Pc* or *E(z)* dsRNA, and mid- and hind-legs were cut at the coxa two days after. (A–D) Larval legs after two molts post dsRNA injection. Center and right panels show close-ups of mid- and hind-legs, respectively. All images in the left column were taken at the same magnification; images in the center and right columns were taken at the same magnification. *Pc* knockdown resulted in larvae with variable degrees of regeneration: some exhibited no regeneration (B) while others partially regenerated (C). Arrowheads point to regenerating legs. (E) Ventral phenotype of *Pc* knockdown pupa that survived pupation after two larval molts. Limbs on the right side of the pupa (left side on the image) are uncut contralateral control legs. Both the midleg and hindleg are missing from the left side of the pupa (arrowheads).

ablated at the femur whereas the hindleg was ablated at the level of the coxa. In addition, to see if the observed regeneration defect is unique to legs, one of the antennae of the same larva was also removed close to the base. The phenotype after two larval molts was recorded (Table 3).

amp^r dsRNA-injected larvae regenerated nearly perfect midlegs after the second molt. The hindleg of *amp*^{r} dsRNA-injected larvae also regenerated all segments although the morphology was distorted (Fig. 9A). *amp*^{r} dsRNA-injected larvae also regenerated their antennae, more or less restoring the original morphology (Fig. 9F).

Midlegs of *Pc* knockdown larvae amputated at the level of the femur were able to regenerate after two molts even when the hindlegs failed to regenerate (Fig. 9B; Table 3). In some of the weakly affected larvae, the midlegs regenerated a normal claw, and all the segments were restored (Fig. 9C). Eight out of 13 larvae failed to regenerate a limb when the hindleg was ablated at the coxa, perhaps because the open wound area is much greater when the limbs are ablated at the coxa; when the femur is cut, the wound margins are often pinched close after ablation and do not remain open. In many *Pc* knockdown larvae, the antennae failed to regenerate properly and only formed a bump (n = 6/13; Fig. 9G). In other *Pc* knockdown larvae, the antennae regenerated a limb that resembled a leg with a claw at the distal end (n = 7/13; Fig. 9H). Thus, *Pc* likely maintains antennal identity during regeneration.

In *E(z)* knockdown larvae, limbs failed to regenerate properly even when they were ablated at the femur. In the most severely affected larvae, the wound had healed, but no new segment was visible (Fig. 9D). In other larvae, a bump resembling a blastema was observed with an occasional pointed tip, but no properly patterned segments were observed (Fig. 9E). The antennae also failed to regenerate and even in the weakly affected larvae, only a single enlarged bump-like structure was observed (Fig. 9I and J). Together, these results demonstrate that Pc and E(z) are necessary for proper re-differentiation of larval appendages and indicate that PcG proteins play extensive roles during limb regeneration in *Tribolium*.

4. Discussion

In this study, the roles of epigenetic histone modifiers, *Pc* and *E(z)*, were examined during metamorphosis and larval leg regeneration through RNA interference. *Pc* and *E(z)* knockdown animals developed abnormal pharate adult morphologies including disrupted eye development and homeotic transformations of legs and wings. Each knockdown produced unique morphologies, indicating that E(z) and Pc play distinct roles during metamorphosis. Furthermore, when *Pc* expression was silenced, limited regeneration was observed at the sites of ablated larval appendages and transformation of the regenerated antenna into a leg. Knockdown of *E(z)* resulted in the complete inhibition of limb re-differentiation. Together, these results demonstrate that *Pc* and *E(z)* play critical roles during post-embryonic sequential ontogenetic plasticity and limb regeneration.

4.1. *Pc* and E(z) maintain segmental identity during metamorphosis

When *Pc* was silenced, we observed homeotic transformations of legs and wings from a mesothoracic (T2) identity to a metathoracic (T3) identity. Similarly, knockdown of *E(z)* led to pharate adults with similar legs on all three thoracic segments and similar fore- and hindwings. We found that *Ubx* is misexpressed in T2 when either *Pc* or *E(z)* is knocked down. Because *Ubx* has been shown to promote hindwing identity during *Tribolium* metamorphosis (Tomoyasu et al., 2005), the upregulation of *Ubx* likely confers T3-like characteristics in the T2 segment. Similarly, forewings of *Pc* mutant *Drosophila* also develop haltere-like structures as Ubx is misexpressed in the developing imaginal discs (Cabrera et al., 1985). Interestingly, however, all three pairs of legs in *Pc* mutant *Drosophila* develop sex combs, which normally develop on forelegs (Mollaaghababa et al., 2001). This is in stark contrast to our observation where the fore- and midlegs assumed a hindleg-like morphology.

In *Drosophila* imaginal discs, Hox misexpression appears patchy; that is, not all cells appear to express the same sets of Hox genes (Cabrera et al., 1985). Such patchiness likely explains why the wings are not completely transformed into halteres. *E(z)* knockdown in *Tribolium* may also result in non-uniform misexpression of Hox genes, leading to mosaic

Table 3
Effects of *Pc* and *Ez(z)* knockdown on leg regeneration after femural and antennal ablations. Larvae were injected on day 0 of sixth larval instar. Two days later, a midleg was ablated at the femur, a hindleg was ablated at the coxa and an antenna was ablated near the boundary of the antennifer and the scapus. Phenotypes after two molts were recorded.

Targeted gene	Total nr	Died after 1 molt	Prepupated after 1 molt	Underwent a second larval-larval molt	Nr with midleg that regenerated segments	Nr with midleg that failed to regenerate	Nr with hindleg that regenerated segments	Nr with hindleg that failed to regenerate	Nr with antenna that regenerated normally	Nr with antennae that failed to regenerate	Nr that regenerated a leg instead of an antenna
amp^r	7	0	3	4	4	0	4	0	4	0	0
Pc	16	9	2	5	0	5[a]	0	5[a]	0	5	0
E(z)	15	2	0	13	13	0	5	8	0	6	7

[a] Includes one larva that formed a tiny claw at the tip of the bump.

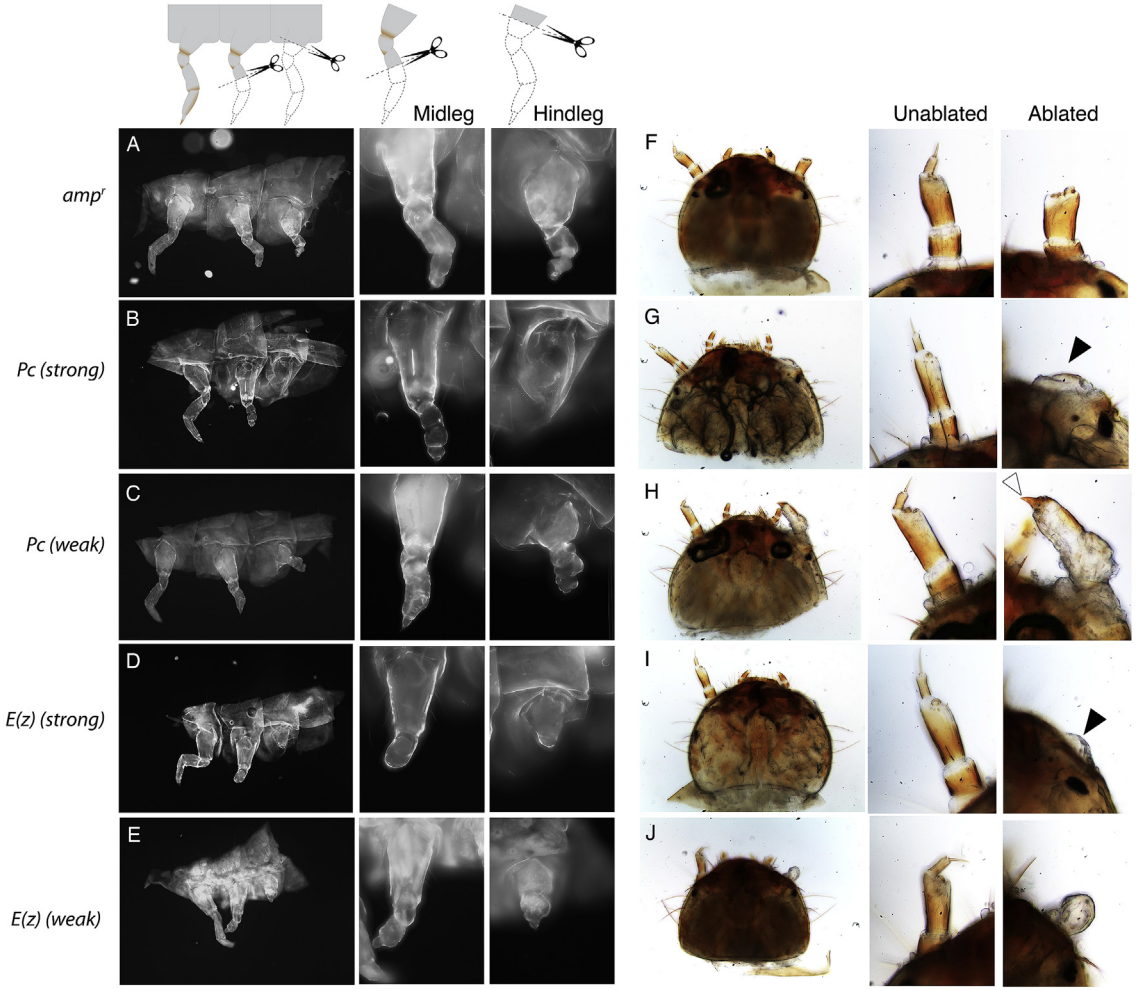

Fig. 9. Pc is necessary for antennal regrowth and antennal specification during regeneration, and E(z) is necessary for both femoral and antennal regeneration. Effects of (A, F) *amp^r*, (B, C, G, H) *Pc* and (D, E, I, J) *E(z)* dsRNA-injection on *Tribolium* femoral and antennal regeneration after two larval molts are shown. Day zero sixth instar larvae were injected with 2 μg/μL *amp^r*, *Pc* or *E(z)* dsRNA. The mid- and hind-legs were cut at the femur and coxa, respectively, two days later. Antennae were also ablated in the same animal. (A–E) Effect of knockdowns on leg regeneration. Middle panels show close-up of mid-legs that were ablated at the femur. Right panels show legs in the same animals that were ablated at the coxa. (F–J) Effect of knockdowns on antennal regeneration. The antennae were ablated near the boundary of the antennifer and the scapus. Middle and right panels show close-up of the unablated antennae and ablated antennae after two molts. (A, F) Effects of ablations in *amp^r* dsRNA-injected larvae. (B, G) Effect of *Pc* knockdown in a strongly affected larva, which failed to regenerate the hindleg and the antenna (black arrowhead). (C, H) Effect of *Pc* knockdown in a weakly affected larva. Legs regenerated, and antenna regenerated a leg-like appendage (open arrowhead). (D, I) Effect of *E(z)* knockdown in a strongly affected larva, which failed to regenerate both legs and antenna (black arrowhead). (E, J) Effect of *E(z)* knockdown in a weakly affected larva. The legs regenerated a small bump at the tip, and antenna regenerated a single enlarged bump-like structure.

wings that exhibit both fore- and hindwing identities. In addition, we observed homeotic transformations of head appendages and the abdomen, indicating that Hox genes become misexpressed in other segments, not just in T2. Together, our findings indicate that PcG proteins maintain spatially restricted Hox gene patterns in metamorphosizing appendages when their imaginal precursor cells undergo dramatic developmental changes to transform the larval appendages into adult appendages (Fig. 10). Notably, with the exception of the terminal segment of the abdomen, and possibly the head, the body wall morphology does not appear to undergo dramatic homeotic

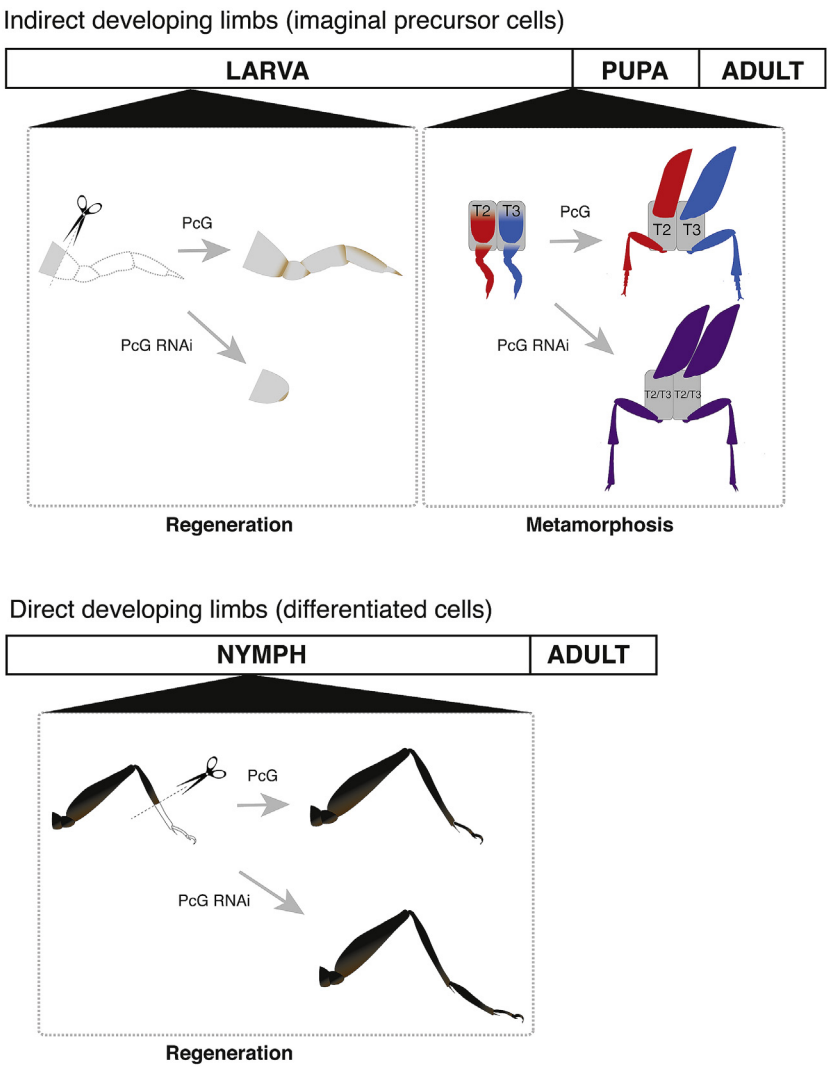

Fig. 10. Proposed roles of PcG proteins in insects with imaginal precursor cells and those with direct limb development. (Top) PcG proteins play critical roles during leg regeneration of *Tribolium*, and their removal prevents legs from re-differentiating. In addition, PcG proteins play critical roles in establishing segmental identity and other major developmental events during metamorphosis (phenotype of *E(z)* knockdown is shown). Homeotic transformations (T2- > T2/T3 transformation is shown) are observed when these genes are silenced during metamorphosis. Thus, PcG proteins play extensive roles in mediating developmental switches and regeneration of insects with imaginal precursor cells. (Bottom) PcG proteins regulate re-patterning of nymphal legs in *Gryllus* but not re-differentiation. Removal of *E(z)* leads to the duplication of the tibial segment. PcG proteins appear to play less extensive roles in these insects with directly-developing limbs.

transformations (Fig. 2), indicating that the roles of PcG proteins are mostly confined to imaginal precursor cells.

It is clear that besides impacting segmental identity, Pc and E(z) both play additional roles. Compound eye development is disrupted in both *Pc* and *E(z)* knockdown animals. In *Drosophila*, analysis of *Pc* and *E(z)* mosaic mutant eye discs showed that these genes are necessary for photoreceptor differentiation at the morphogenetic furrow or at the posterior margin (Janody et al., 2004). Functions of these genes may be conserved between the two species. In addition, in *E(z)* knockdown *Tribolium*, the head appendages developed single elongated segments that lacked the normal number of segments. We suspect that E(z) normally represses critical regulators that are directly or indirectly involved in the establishment of appendage segment identities. Finally, the wings were much smaller in *E(z)* knockdown adults. We suspect that E(z) plays a role in wing imaginal cell proliferation during the prepupal period.

4.2. Potential roles of Pc and E(z) in repressing re-differentiation genes

Because wound healing and at least a small bump was observed after limb ablation in *Pc* and *E(z)* knockdown larvae (Fig. 8), we infer that wound healing does not require Pc or E(z). Instead, the re-differentiation step appears to be impaired, permanently maintaining the blastema stage. Because Pc and E(z) are part of the PcG proteins, which are a set of general transcriptional repressors, we propose two different hypotheses for the observed lack of regeneration. First, it is possible that these PcG proteins actively repress blastema-specific genes during the re-differentiation step and that their de-repression leads to the permanent maintenance of blastemas. Alternatively, it is possible that Pc and E(z) are necessary for repressing differentiation signals and/or maintaining the proliferative state of blastemal cells: without E(z) or Pc, blastemal cells stop proliferating and/or undergo premature differentiation. Curiously, when *Pc* was silenced, the midleg ablated at the femur was able to regenerate even when the hindleg, ablated at the coxa, was unable to do so in the same larva (Fig. 8B). This may be due to the fact that not as many cells are needed to recreate the limb when the femur is ablated; this explanation would be consistent with the idea that *Pc* knockdown leads to premature differentiation. In regenerating *Drosophila* imaginal discs, *Pc* is downregulated in response to JNK signaling, a wound healing pathway (Lee et al., 2005). This decline is associated with the activation of *wingless* (*wg*), which plays key roles in blastema formation and transdetermination of imaginal discs, indicating that the decline in Pc allows cells to de-differentiate to acquire multipotency (Lee et al., 2005). While this has not been investigated, it is possible that Pc may subsequently need to be re-expressed in order for the imaginal discs to re-differentiate. In addition, our study indicates that at least Pc is necessary for maintaining the segmental identity of antennae as silencing of *Pc* led to the regeneration of a leg-like structure in some larvae (Fig. 9C). Thus, similar to *Drosophila*, Pc removal appears to be associated with an increased frequency of transdetermination (Lee et al., 2005), possibly mediated by Hox gene misexpression as observed during metamorphosis.

Mammalian stem cells have demonstrated similar roles for EZH2. In mice muscles, EZH2 is expressed in quiescent satellite cells and is necessary for homeostatic maintenance of the adult quiescent satellite pool (Juan et al., 2011; Palacios et al., 2010). When EZH2 is experimentally reduced, the number of satellite cells decreases and muscle regeneration is impaired because EZH2 is necessary for maintaining the proliferative capacity of satellite cell pool. In addition, EZH2 has been shown to be necessary for permitting the differentiation of muscle cells by repressing Pax7, a satellite cell specific transcription factor (Juan et al., 2011; Palacios et al., 2010). Epidermal stem cells also express EZH2, and its expression is necessary for maintaining the proliferative potential of stem cells and preventing premature differentiation of epidermis (Ezhkova et al., 2009). Finally, multipotent progenitor cells of the cerebral cortex have also been shown to require EZH2 for their proliferation and inhibition of premature differentiation (Pereira et al., 2010).

4.3. Comparison with epigenetic regulation of regeneration in other organisms

A role for H3K27 methylation during regeneration has also been demonstrated in zebrafish. In zebrafish, the H3K27 demethylase KDM6 is necessary for regeneration in adult caudal fins (Stewart et al., 2009). During larval fin regeneration, EZH2 has also been shown to be necessary for regeneration (Dupret et al., 2017). One interpretation is that blastemal formation and initiation of regeneration requires demethylation of H3K27, whereas subsequent re-differentiation requires PRC2-dependent H3K27 methylation. Alternatively, histone modifiers may play different roles during regeneration of larval versus adult fins. Regardless, regeneration of zebrafish fins requires EZH2, similar to *Tribolium* legs.

Our finding that *E(z)* knockdown in *Tribolium* leads to a loss of regenerative ability is different from what is observed during leg regeneration in cricket nymphal legs. In *Gryllus*, knockdown of *E(z)* results in re-differentiated legs that contain an additional tibia-like segment (Hamada et al., 2015) (Fig. 10). This curious difference may arise from the fact that cricket nymphal legs are more fully developed at the time of regeneration whereas larval legs are still incompletely differentiated. In fact, we have shown that in *Tribolium*, these genes play major roles during metamorphosis to specify both the appendage morphology and identity (Figs. 3–7), whereas no such transformations were noted during post-embryonic development of *Gryllus* (Hamada et al., 2015). Thus, the timing of epigenetic regulation in limb development appears to be heterochronically shifted to a later stage of development in holometabolous insects: at the time of ablation, the cells in the larval legs have undergone less differentiation than *Gryllus* nymphal legs (Truman and Riddiford, 2002; Villarreal et al., 2015), and the relative importance of chromatin structure may differ between the juveniles of the two species (Fig. 10).

Taken together, we hypothesize that during regeneration involving incompletely differentiated limbs derived from imaginal precursor cells, histone methylation may play a critical role, specifically during proliferation of precursor cells and/or blastemal formation. In contrast, regeneration of differentiated structures, as seen in cricket legs, may not require histone modification for blastemal formation and cell proliferation. Studies from additional taxa should help clarify the extent to which the distinct functions reflect differences in life cycles (i.e., hemimetabolous versus holometabolous, and differences in timing of appendage development) of these insects, or divergences in the functions of PcG genes themselves.

5. Conclusions

Our study demonstrates that epigenetic regulators play critical roles during both metamorphosis and regeneration. Specifically, our study demonstrates that E(z) and Pc play both conserved and distinct roles during metamorphosis to maintain proper segmental identities. The functions of PcG proteins during embryogenesis have been well characterized. Our findings demonstrate that the dramatic rearrangements and remodeling of larval structures during metamorphosis mark the second phase of development when epigenetic regulators play critical roles in maintaining proper expression of genes. PcG genes also play critical roles in *Tribolium* leg regeneration. Together, these findings indicate that PcG proteins play extensive roles in regulating plasticity of imaginal precursor cells.

Acknowledgements

We thank the three anonymous reviewers for their constructive feedback on the manuscript. We also thank Drs. Melissa Beers and Adam Matthews for their critical reading of the early drafts of the manuscript and the members of the Suzuki lab for their helpful discussions and assistance. This work was supported in part by grants from Wellesley College and the National Science Foundation IOS-1027453 and IOS-1354608 to Y.S.

Appendix A. Supplementary data

Supplementary data to this article can be found online at https://doi.org/10.1016/j.ydbio.2019.03.002.

References

Akasaka, T., Kanno, M., Balling, R., Mieza, M.A., Taniguchi, M., Koseki, H., 1996. A role for mel-18, a Polycomb group-related vertebrate gene, during the anteroposterior specification of the axial skeleton. Development 122, 1513–1522.
Aloia, L., Di Stefano, B., Di Croce, L., 2013. Polycomb complexes in stem cells and embryonic development. Development 140, 2525–2534.
Bel, S., Core, N., Djabali, M., Kieboom, K., Van der Lugt, N., Alkema, M.J., Van Lohuizen, M., 1998. Genetic interactions and dosage effects of Polycomb group genes in mice. Development 125, 3543–3551.
Brockes, J.P., 1997. Amphibian limb regeneration: rebuilding a complex structure. Science 276, 81–87.
Cabrera, C.V., Botas, J., Garciabellido, A., 1985. Distribution of Ultrabithorax proteins in mutants of Drosophila bithorax complex and its transregulatory genes. Nature 318, 569–571.
Cao, R., Wang, L.J., Wang, H.B., Xia, L., Erdjument-Bromage, H., Tempst, P., Jones, R.S., Zhang, Y., 2002. Role of histone H3 lysine 27 methylation in polycomb-group silencing. Science 298, 1039–1043.
Cao, R., Zhang, Y., 2004. The functions of E(Z)/EZH2-mediated methylation of lysine 27 in histone H3. Curr. Opin. Genet. Dev. 14, 155–164.
Czermin, B., Melfi, R., McCabe, D., Seitz, V., Imhof, A., Pirrotta, V., 2002. Drosophila enhancer of Zeste/ESC complexes have a histone H3 methyltransferase activity that marks chromosomal Polycomb sites. Cell 111, 185–196.
Di Croce, L., Helin, K., 2013. Transcriptional regulation by Polycomb group proteins. Nat. Struct. Mol. Biol. 20, 1147–1155.
Dupret, B., Volkel, P., Vennin, C., Toillon, R.A., Le Bourhis, X., Angrand, P.O., 2017. The histone lysine methyltransferase Ezh2 is required for maintenance of the intestine integrity and for caudal fin regeneration in zebrafish. Biochim. Biophys. Acta Gene Regul. Mech. 1860, 1079–1093.
Echeverri, K., Tanaka, E.M., 2002. Mechanisms of muscle dedifferentiation during regeneration. Semin. Cell Dev. Biol. 13, 353–360.
Endo, T., Bryant, S.V., Gardiner, D.M., 2004. A stepwise model system for limb regeneration. Dev. Biol. 270, 135–145.
Endoh, M., Endo, T.A., Endoh, T., Isono, K., Sharif, J., Ohara, O., Toyoda, T., Ito, T., Eskeland, R., Bickmore, W.A., et al., 2012. Histone H2A mono-ubiquitination is a crucial step to mediate PRC1-dependent repression of developmental genes to maintain ES cell identity. PLoS Genet. 8, e1002774.
Ezhkova, E., Pasolli, H.A., Parker, J.S., Stokes, N., Su, I.H., Hannon, G., Tarakhovsky, A., Fuchs, E., 2009. Ezh2 orchestrates gene expression for the stepwise differentiation of tissue-specific stem cells. Cell 136, 1122–1135.
Francis, N.J., Saurin, A.J., Shao, Z., Kingston, R.E., 2001. Reconstitution of a functional core polycomb repressive complex. Mol. Cell 8, 545–556.
Glicksman, M.A., Brower, D.L., 1988. Misregulation of homeotic gene-expression in Drosophila larvae resulting from mutations at the extra sex combs locus. Dev. Biol. 126, 219–227.
Grossniklaus, U., Paro, R., 2014. Transcriptional silencing by polycomb-group proteins. Cold Spring Harb. Perspect. Biol. 6, a019331.
Gutierrez, L., Oktaba, K., Scheuermann, J.C., Gambetta, M.C., Ly-Hartig, N., Muller, J., 2012. The role of the histone H2A ubiquitinase Sce in Polycomb repression. Development 139, 117–127.
Hamada, Y., Bando, T., Nakamura, T., Ishimaru, Y., Mito, T., Noji, S., Tomioka, K., Ohuchi, H., 2015. Leg regeneration is epigenetically regulated by histone H3K27 methylation in the cricket Gryllus bimaculatus. Development 142, 2916–2927.
Hayashi, S., Kawaguchi, A., Uchiyama, I., Kawasumi-Kita, A., Kobayashi, T., Nishide, H., Tsutsumi, R., Tsuru, K., Inoue, T., Ogino, H., et al., 2015. Epigenetic modification

maintains intrinsic limb-cell identity in Xenopus limb bud regeneration. Dev. Biol. 406, 271–282.
Huet, C., Lenoir-Rousseaux, J.J., 1976. Etude de la mise en place de la patte imaginable de Tenebrio molitor. 1. Analyse expérimentale des processus de restauration au cours de la morphogenése. J. Embryol. Exp. Morphol. 35, 303–321.
Hughes, C.L., Kaufman, T.C., 2000. RNAi analysis of Deformed, proboscipedia and Sex combs reduced in the milkweed bug Oncopeltus fasciatus: novel roles for Hox genes in the Hemipteran head. Development 127, 3683–3694.
Janody, F., Lee, J.D., Jahren, N., Hazelett, D.J., Benlali, A., Miura, G.I., Draskovic, I., Treisman, J.E., 2004. A mosaic genetic screen reveals distinct roles for trithorax and polycomb group genes in Drosophila eye development. Genetics 166, 187–200.
Jones, R.S., Gelbart, W.M., 1990. Genetic-analysis of the enhancer of zeste locus and its role in gene-regulation in Drosophila-melanogaster. Genetics 126, 185–199.
Juan, A.H., Derfoul, A., Feng, X., Ryall, J.G., Dell'Orso, S., Pasut, A., Zare, H., Simone, J.M., Rudnicki, M.A., Sartorelli, V., 2011. Polycomb EZH2 controls self-renewal and safeguards the transcriptional identity of skeletal muscle stem cells. Genes Dev. 25, 789–794.
Jurgens, G., 1985. A group of genes controlling the spatial expression of the bithorax complex in Drosophila. Nature 316, 153–155.
Katsuyama, T., Paro, R., 2011. Epigenetic reprogramming during tissue regeneration. FEBS Lett. 585, 1617–1624.
Klymenko, T., Papp, B., Fischle, W., Kocher, T., Schelder, M., Fritsch, C., Wild, B., Wilm, M., Muller, J., 2006. A Polycomb group protein complex with sequence-specific DNA-binding and selective methyl-lysine-binding activities. Genes Dev. 20, 1110–1122.
Konstantinides, N., Averof, M., 2014. A common cellular basis for muscle regeneration in arthropods and vertebrates. Science 343, 788–791.
Kragl, M., Knapp, D., Nacu, E., Khattak, S., Maden, M., Epperlein, H.H., Tanaka, E.M., 2009. Cells keep a memory of their tissue origin during axolotl limb regeneration. Nature 460, 60–U69.
Lee, N., Maurange, C., Ringrose, L., Paro, R., 2005. Suppression of Polycomb group proteins by JNK signalling induces transdetermination in Drosophila imaginal discs. Nature 438, 234–237.
Lewis, E.B., 1978. A gene complex controlling segmentation in Drosophila. Nature 276, 565–570.
Lewis, P.H., 1947. Melanogaster new mutants: report of Pamela H. Lewis. Drosoph. Inf. Serv. 21, 69.
Maruzzo, D., Bortolin, F., 2013. Arthropod regeneration. In: Minelli, Alessandro, Boxshall, Geoffrey, Fusco, Giuseppe (Eds.), Arthropod Biology and Evolution. Springer, Berlin, Heidelberg.
Matsuoka, Y., Bando, T., Watanabe, T., Ishimaru, Y., Noji, S., Popadic, A., Mito, T., 2015. Short germ insects utilize both the ancestral and derived mode of Polycomb group-mediated epigenetic silencing of Hox genes. Biol. Open 4, 702–709.
McKeon, J., Brock, H.W., 1991. Interactions of the Polycomb group of genes with homeotic loci of Drosophila. Roux. Arch. Dev. Biol. 199, 387–396.
Mitten, E.K., Jing, D., Suzuki, Y., 2012. Matrix metalloproteinases (MMPs) are required for wound closure and healing during larval leg regeneration in the flour beetle, Tribolium castaneum. Insect Biochem. Molec. 42, 854–864.
Mollaaghababa, R., Sipos, L., Tiong, S.Y.K., Papoulas, O., Armstrong, J.A., Tamkun, J.W., Bender, W., 2001. Mutations in Drosophila heat shock cognate 4 are enhancers of polycomb. Proc. Natl. Acad. Sci. U.S.A. 98, 3958–3963.
Muller, J., Bienz, M., 1991. Long-range repression conferring boundaries of Ultrabithorax expression in the Drosophila embryo. EMBO J. 10, 3147–3155.
Muller, J., Hart, C.M., Francis, N.J., Vargas, M.L., Sengupta, A., Wild, B., Miller, E.L., O'Connor, M.B., Kingston, R.E., Simon, J.A., 2002. Histone methyltransferase activity of a Drosophila Polycomb group repressor complex. Cell 111, 197–208.
Palacios, D., Mozzetta, C., Consalvi, S., Caretti, G., Saccone, V., Proserpio, V., Marquez, V.E., Valente, S., Mai, A., Forcales, S.V., et al., 2010. TNF/p38alpha/polycomb signaling to Pax7 locus in satellite cells links inflammation to the epigenetic control of muscle regeneration. Cell Stem Cell 7, 455–469.
Pengelly, A.R., Copur, O., Jackle, H., Herzig, A., Muller, J., 2013. A histone mutant reproduces the phenotype caused by loss of histone-modifying factor polycomb. Science 339, 698–699.
Pereira, J.D., Sansom, S.N., Smith, J., Dobenecker, M.W., Tarakhovsky, A., Livesey, F.J., 2010. Ezh2, the histone methyltransferase of PRC2, regulates the balance between self-renewal and differentiation in the cerebral cortex. P Natl. Acad. Sci. USA 107, 15957–15962.
Ringrose, L., Paro, R., 2004. Epigenetic regulation of cellular memory by the Polycomb and Trithorax group proteins. Annu. Rev. Genet. 38, 413–443.
Rouhana, L., Tasaki, J., 2016. Epigenetics and shared molecular processes in the regeneration of complex structures. Stem Cell. Int. 2016, 6947395. https://doi.org/10.1155/2016/6947395.
Sandoval-Guzman, T., Wang, H., Khattak, S., Schuez, M., Roensch, K., Nacu, E., Tazaki, A., Joven, A., Tanaka, E.M., Simon, A., 2014. Fundamental differences in dedifferentiation and stem cell recruitment during skeletal muscle regeneration in two salamander species. Cell Stem Cell 14, 174–187.
Sauvageau, M., Sauvageau, G., 2010. Polycomb group proteins: multi-faceted regulators of somatic stem cells and cancer. Cell Stem Cell 7, 299–313.
Schuettengruber, B., Bourbon, H.M., Di Croce, L., Cavalli, G., 2017. Genome regulation by polycomb and trithorax: 70 Years and counting. Cell 171, 34–57.
Shah, M.V., Namigai, E.K., Suzuki, Y., 2011. The role of canonical Wnt signaling in leg regeneration and metamorphosis in the red flour beetle Tribolium castaneum. Mech. Dev. 128, 342–358.
Shao, Z., Raible, F., Mollaaghababa, R., Guyon, J.R., Wu, C.T., Bender, W., Kingston, R.E., 1999. Stabilization of chromatin structure by PRC1, a Polycomb complex. Cell 98, 37–46.
Simon, J., Chiang, A., Bender, W., 1992. Ten different Polycomb group genes are required for spatial control of the abdA and AbdB homeotic products. Development 114, 493–505.
Smith, F.W., Jockusch, E.L., 2014. Hox genes require homothorax and extradenticle for body wall identity specification but not for appendage identity specification during metamorphosis of Tribolium castaneum. Dev. Biol. 395, 182–197.
Snodgrass, R.E., 1954. Insect metamorphosis. Smithsonian Misc. Collect. 122 (9), 84.
Stewart, S., Tsun, Z.Y., Belmonte, J.C.I., 2009. A histone demethylase is necessary for regeneration in zebrafish. Proc. Natl. Acad. Sci. U.S.A. 106, 19889–19894.
Struhl, G., 1981. A gene product required for correct initiation of segmental determination in Drosophila. Nature 293, 36–41.
Takihara, Y., Tomotsune, D., Shirai, M., Katoh-Fukui, Y., Nishii, K., Motaleb, M.A., Nomura, M., Tsuchiya, R., Fujita, Y., Shibata, Y., et al., 1997. Targeted disruption of the mouse homologue of the Drosophila polyhomeotic gene leads to altered anteroposterior patterning and neural crest defects. Development 124, 3673–3682.
Tanaka, K., Truman, J.W., 2005. Development of the adult leg epidermis in Manduca sexta: contribution of different larval cell populations. Dev. Gene. Evol. 215, 78–89.
Tomoyasu, Y., Wheeler, S.R., Denell, R.E., 2005. Ultrabithorax is required for membranous wing identity in the beetle Tribolium castaneum. Nature 433, 643–647.
Truman, J.W., Riddiford, L.M., 2002. Endocrine insights into the evolution of metamorphosis in insects. Annu. Rev. Entomol. 47, 467–500.
van der Lugt, N.M., Domen, J., Linders, K., van Roon, M., Robanus-Maandag, E., te Riele, H., van der Valk, M., Deschamps, J., Sofroniew, M., van Lohuizen, M., et al., 1994. Posterior transformation, neurological abnormalities, and severe hematopoietic defects in mice with a targeted deletion of the bmi-1 proto-oncogene. Genes Dev. 8, 757–769.
Villarreal, C.M., Darakananda, K., Wang, V.R., Jayaprakash, P.M., Suzuki, Y., 2015. Hedgehog signaling regulates imaginal cell differentiation in a basally branching holometabolous insect. Dev. Biol. 404, 125–135.
Wang, H., Wang, L., Erdjument-Bromage, H., Vidal, M., Tempst, P., Jones, R.S., Zhang, Y., 2004a. Role of histone H2A ubiquitination in Polycomb silencing. Nature 431, 873–878.
Wang, L., Brown, J.L., Cao, R., Zhang, Y., Kassis, J.A., Jones, R.S., 2004b. Hierarchical recruitment of polycomb group silencing complexes. Mol. Cell 14, 637–646.